J Mol Model (2012) 18:4409–4415
DOI 10.1007/s00894-012-1451-y

ORIGINAL PAPER

Rational design of a nitrite reductase based on myoglobin: a molecular modeling and dynamics simulation study

Ying-Wu Lin · Chang-Ming Nie · Li-Fu Liao

Received: 10 December 2011 / Accepted: 30 April 2012 / Published online: 16 May 2012

Abstract Myoglobin (Mb) is an ideal scaffold protein for rational protein design mimicking native enzymes. We recently designed a nitrite reductase (NiR) based on sperm whale Mb by introducing an additional distal histidine (Leu29 to His29 mutation) and generating a distal tyrosine (Phe43 to Tyr43 mutation) in the heme pocket, namely L29H/F43Y Mb, to mimic the active site of cytochrome cd_1 NiR from *Ps. aeruginosa* that contains two distal histidines and one distal tyrosine. The molecular modeling and dynamics simulation study herein revealed that L29H/F43Y Mb has the necessary structural features of native cytochrome cd_1 NiR and can provide comparable interactions with nitrite as in native NiRs, which provides rationality for the protein design and guides the protein engineering. Additionally, the present study provides an insight into the relatively low NiR activity of Mb in biological systems.

Keywords Denitrification · MD simulation · Myoglobin · Nitrite reductase · Protein design

Introduction

Myoglobin (Mb) is a single-chain globular protein of ~153 amino acids, which contains a heme group and functions as an oxygen carrier [1–3]. Notably, to address important issues in chemistry and biology, Mb has been successfully used as an ideal scaffold protein for rational design of both structural and functional proteins mimicking native enzymes [4–6], such as heme-copper oxidase (HCO) [7–9] and nitric oxide reductase (NOR) [10–13]. Compared to the traditional approach of the study of native enzymes [14–17], the rational design of biomimetic models using Mb offers incomparable advantages, such as being much smaller, easier to express in high yields, and free of other chromophores [4–12].

Aside from NOR that catalyzes reduction of NO to N_2O ($2NO + 2H^+ + 2e^- \rightarrow N_2O + H_2O$) [18], nitrite reductase (NiR) is another crucial enzyme involved in the bacterial denitrification pathway by catalyzing reduction of NO_2^- to NO ($NO_2^- + 2H^+ + e^- \rightarrow NO + H_2O$) [19–24]. Actually, the product of NiR, NO, is the substrate of NOR, and both enzymes are heme proteins. Cytochrome cd_1 (cyt cd_1) NiR from *Ps. aeruginosa* is one of the most studied NiRs, which contains 543 amino acids and forms a homodimer, with one heme *c* and one heme d_1 in each subunit (Fig. 1) [19–24]. Electrons are transferred from cytochrome c_{551} to the heme *c* of the enzyme [25], and thereby to the active site of heme d_1, to which the substrate NO_2^- binds and is reduced to NO [19–24]. The X-ray crystal structure shows that two distal histidines (His327 and His369) and one tyrosine (Y10) from the other monomer interact with the heme d_1 axial water molecule (Fig. 1) [22], and these residues are found to be essential for NiR activity [19–24].

Like NOR, the properties of cyt cd_1 NiR such as high molecular weight and many heme centers limit the deep study of the native enzyme and ultimate applications. The successful design of NOR using sperm whale Mb as a scaffold protein prompted us to further design of a NiR based on Mb. It is interesting and challenging to design

Y.-W. Lin (✉) · C.-M. Nie · L.-F. Liao
School of Chemistry and Chemical Engineering,
University of South China,
Hengyang 421001, China
e-mail: linlinying@hotmail.com

Y.-W. Lin
State Key Laboratory of Coordination Chemistry,
Nanjing University,
Nanjing 210093, China

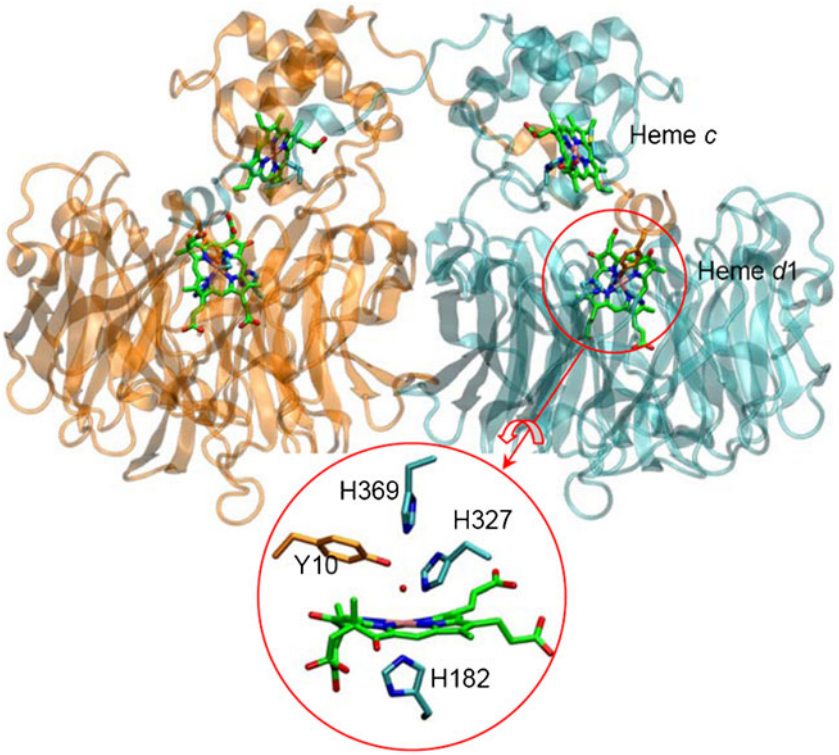

Fig. 1 X-ray crystal structure of cyt cd_1 NiR from *Ps. aeruginosa* (PDB entry 1NIR), showing the homodimer. The heme *c* and *d*1 centers are highlighted. The heme *d*1 active center is zoomed in for clarification

two close-related enzymes, NOR and NiR, by using the same protein scaffold of Mb. Another motivation is that native Mb was also found to exhibit low NiR activity [26–30] and should be a good start point. As for NOR design [10], we used computer modeling in combination with molecular dynamics (MD) simulations to search for suitable target residues for modifications. Finally, we designed a L29H/F43Y Mb mutant in which an additional distal histidine was introduced at position 29 and the distal Phe43 was mutated to a tyrosine residue, and the confirmation of NiR activity enhancement using both spectroscopic and electronic methods is currently under progress. As a theoretical study, we report herein the rationality of the design of L29H/F43Y Mb, the simulated protein structure and its nitrite complex, as well as the dynamics property of nitrite binding to the designed protein.

Methods

The structure of L29H/F43Y Mb in the ferric state was modeled based on the X-ray crystal structure of sperm whale Mb (PDB entry 1JP6 [31]), including the heme axial water molecule. Leu29 and Phe43 were first mutated to His and Tyr, respectively, using program VMD 1.9 (Visual Molecular Dynamics) [32]. The psfgen plug-in of program NAMD 2.7 (Nanoscale Molecular Dynamics) [33] was used to add hydrogen atoms and assign charges to L29H/F43Y Mb, which was set up according to pH 7. The distal histidines, His64 and His29, were modeled with hydrogen at the δ-position. The protein was solvated in a cubic box of TIP3 water, which extended 10 Å away from any given protein atom. A total of 19 counter ions (9 Na^+ and 10 Cl^-) were further added to the system to obtain the physiological ionic strength of 0.15 M by using the autoionize plug-in of VMD 1.9. The resulting system was minimized with NAMD 2.7 by employing the classical force filed CHARMM27 [34], using 5000 minimization steps with conjugate gradient method at 0 K, and equilibrated for 10,000 molecular dynamics steps (1 fs per step) via an NVT ensemble (where the number of particles N, the volume V, and the temperature T of the system are kept constant) at 300 K, then further minimized for 5000 steps for analysis with VMD 1.9, similar to the previous report on modeling of L29H/F43H/V68E Mb mutant [10].

In order to model nitrite binding to L29H/F43Y Mb, the heme axial water molecule was replaced by a nitrite anion, and the two distal histidine residues, His29 and His64, were considered charged, i.e., protonated at both N_δ and N_ε, as in the previous study [35]. An O-bound model was simulated for NO_2^- based on experimental observation that the distal His64 directs nitrite binding to the heme iron [36], and an atomic charge of O_1 (−0.43 e) was used for the nitrite anion according to the previous calculation [35]. The nitrite-protein system was then equilibrated using the same procedure as described above. To probe the dynamic property of nitrite binding to L29H/F43Y Mb, the simulated complex of L29H/F43Y Mb- NO_2^- was subsequently subjected to a MD simulation with program NAMD 2.7 at 300 K for 10 ns. The

Langevin dynamics was used for constant temperature control, with the Langevin coupling coefficient set to 5 ps. The trajectory data was saved every 10,000 steps (corresponding to 10 ps), generating 1000 structures over 10 ns of simulation. A control simulation was performed for NO_2^- binding to WT Mb under the same condition. Each simulation was repeated, resulting in two separate trajectories for both L29H/F43Y Mb-nitrite and Mb-nitrite systems. The average data were then used for analysis by VMD 1.9.

Results and discussion

Modeling the structure of L29H/F43Y Mb

With energy minimization and equilibration, the simulated structure of L29H/F43Y Mb in the ferric state is shown in Fig. 2a. In comparison to WT Mb in the X-ray crystal structure (PDB entry 1JP6), L29H/F43Y Mb adopts a similar overall structure as simulated in solution, which agrees with the observation that L29H/F43Y Mb has a similar UV-visible spectrum (Soret band, 406 nm and visible band, 630 nm, unpublished data) to that of WT Mb [37], indicating the two mutations do not perturb the protein structure significantly. In the heme distal pocket, both Tyr43 and His64 were found to form hydrogen bonds with the axial water molecule, with a distance of 2.77 Å (tyrosine oxygen and water oxygen) and 2.97 Å (histidine ε-nitrogen and water oxygen), respectively. Meanwhile, the distance between ε-nitrogen (N_ε) of His29 and axial water oxygen is 4.06 Å, indicating there is no direct hydrogen bonding interaction.

When compared to the heme d_1 active center of native cyt cd_1 NiR (PDB entry 1NIR [22]) by spatial alignment (Fig. 2b), it was shown that L29H/F43Y Mb has a very similar heme active site, where both distal histidines and tyrosine have similar spatial positions with respect to that in cyt cd_1 NiR. Although these residues do not overlay very well, it was found that the residues in cyt cd_1 NiR have similar distances to the axial water as those in L29H/F43Y Mb. For example, the distance between Tyr10 oxygen and water oxygen is 2.61 Å, and the distance between ε-nitrogen of His369 and His327 and axial water oxygen is 3.38 Å and 4.69 Å, respectively. These observations suggest that as designed, the L29H/F43Y Mb mutant has the structural features necessary to contribute to the function of native NiR.

Modeling the structure of L29H/F43Y Mb-nitrite complex

Based on the previous finding that the distal His64 of Mb directs the O-binding model of nitrite to the heme iron [36], we simulated NO_2^- binding to L29H/F43Y Mb with its O_1 atom coordinated to the heme iron. As shown in Fig. 3a, with the heme axial water molecule replaced by a NO_2^-, the overall structure of the protein remains intact, in which NO_2^- coordinates to heme iron with a distance of O_1…Fe 2.00 Å after energy minimization and equilibration. The distal His64 and His29 were found to form two hydrogen bonds with O_1 and O_2 atoms of NO_2^-, O_1…H(N_ε-H64) (1.94 Å) and O_2…H(N_ε-H29) (1.69 Å), respectively. Concurrently, the hydroxyl group of Tyr43 was also hydrogen bonded to the nitrite O_2 atom (1.92 Å). These hydrogen bond interactions provided by the key distal residues in L29H/F43Y Mb could therefore contribute to the NiR activity.

As a control study, we simulated NO_2^- binding to WT Mb in the O-bound model (Fig. 3b) and compared with L29H/F43Y Mb-nitrite (Fig. 3c) as well as the X-ray crystal structure of Mb-nitrite complex available from literature (Fig. 3d) [38]. The distal His64 was found to stabilize nitrite through a stable hydrogen bond, O_1…H(N_ε) (1.86 Å), and a weaker hydrogen bond, O_2…H(N_ε) (2.50 Å) as well. This observation agrees with the crystallography study of horse

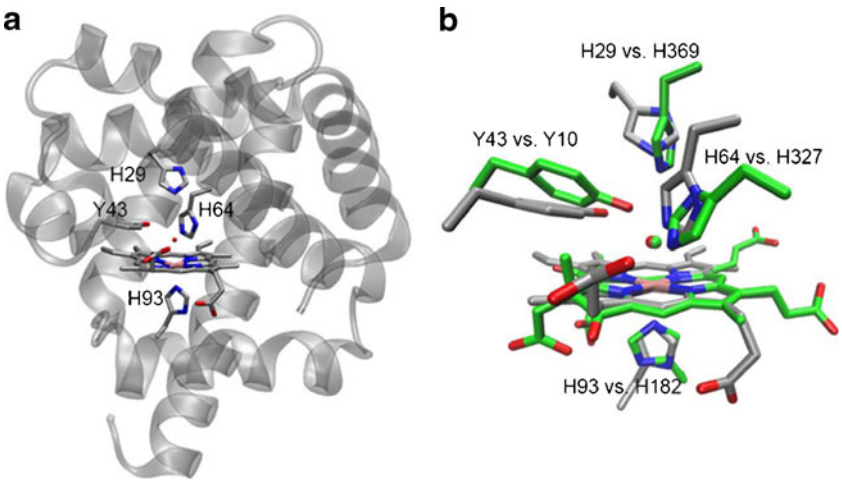

Fig. 2 Modeling structure of L29H/F43Y Mb (**a**) and the overlay with the heme *d*1 active site of cyt cd_1 NiR from *Ps. aeruginosa* (blue) (**b**)

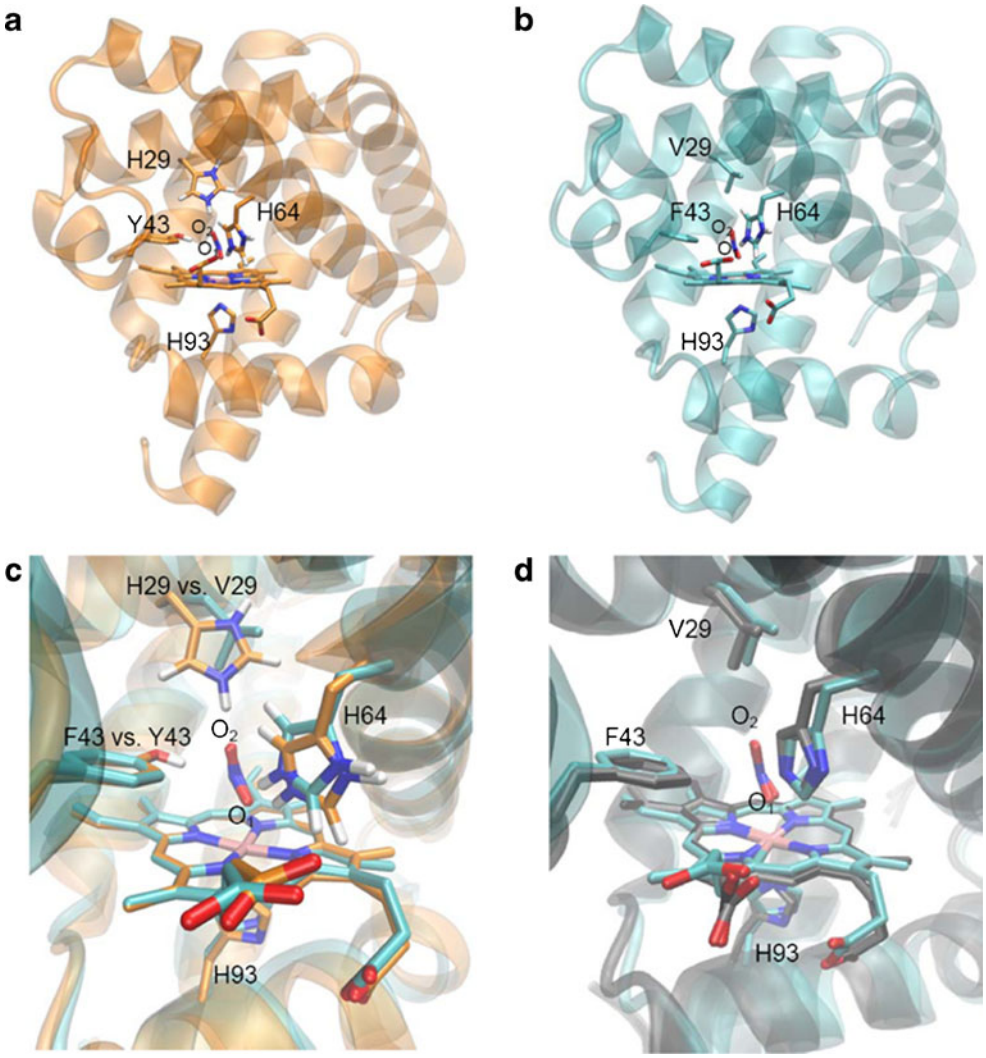

Fig. 3 Modeling structure of L29H/F43Y Mb-nitrite (**a**) and Mb-nitrite (**b**) complexes, and the overlay of each other (**b**). The overlay of Mb-nitrite complex (cyan) with the X-ray crystal structure of horse heart Mb-nitrite complex (black, co-crystallized, PDB entry 2FRI, and gray, crystal soak, PDB entry 2FRF) is shown in (**b**)

heart Mb-nitrite complex that shows the distance of $O_2 \ldots N_\varepsilon$ (His64) (3.13-3.20 Å) is slightly longer than that of $O_1 \ldots N_\varepsilon$ (His64) (2.68-2.83 Å) [38] (Table 1). The overlay of L29H/F43Y Mb-nitrite and WT Mb-nitrite shows that with introduction of a histidine at position 29 and mutation of Phe43 to tyrosine, the conformation of distal His64 changed slightly, meanwhile, the bound nitrite remained in a similar orientation (Fig. 3c), suggesting that L29H/F43Y Mb has a suitable heme distal pocket and readily binds nitrite. On the other hand, as shown in Fig. 3d, the simulated complex of WT Mb-nitrite overlays well with the X-ray crystal structure of horse heart Mb-nitrite complex, validating the present simulation.

Moreover, previous study revealed that both α and β subunits of hemoglobin bind nitrite in the O-bound model [39]. As compared to the present simulation (Table 1), it can be observed that the distal His64 of WT Mb-nitrite and L29H/F43Y Mb-nitrite complexes has similar hydrogen bonding interactions with nitrite as that for distal His58 and His63 in α and β subunits, respectively, with nitrite orientation closer to that in the α subunit. To date, there is no structure report on the complex of cyt cd_1 NiR from *Ps. aeruginosa* with nitrite. Alternatively, the X-ray crystal structure of the N-bound nitrite adduct of cyt cd_1 NiR from *P. pantotrophus* shows that two distal histidines, His345 and His388, form hydrogen bonds with the nitrite O_2 atom, simultaneously (Table 1) [40]. Note that there is no distal tyrosine in this NiR enzyme. In another crystallographic study of cyt *c* NiR [41], the distal His277 and Tyr218 were found to form hydrogen bonds with the nitrite O_1 atom, simultaneously (Table 1), whereas the other distal histidine was replaced by an arginine in this enzyme, and the latter forms an hydrogen bond the O_2 atom of nitrite (2.81 Å). Although nitrite is in an O-bound model, these interactions are quite similar to those seen in the simulation of the L29H/F43Y Mb-nitrite complex, indicating that the designed protein can provide comparable interactions with nitrite as that in native NiRs and is thus a promising artificial NiR.

Table 1 Comparison of the distance between distal histidine(s) or tyrosine and nitrite ion

Protein-NO_2^- complexes	Bound model	Distance (Å)	Method	Ref
WT Mb[a]-NO_2^-	O-bound	(Nitrite) O_1- N_ε (H64): 2.79 (Nitrite) O_2- N_ε (H64): 3.12	MD Simulation	This work
L29H/F43Y Mb[a]-NO_2^-	O-bound	(Nitrite) O_1- N_ε (H64): 2.89 (Nitrite) O_2- N_ε (H29): 2.71 (Nitrite) O_2- O (Y43): 2.77	MD Simulation	This work
WT Mb[b]-NO_2^-	O-bound	(Nitrite) O_1- N_ε (H64): 2.68 (Nitrite) O_2- N_ε (H64): 3.13	Co-crystallized (PDB entry 2FRI)	38
WT Mb[b]-NO_2^-	O-bound	(Nitrite) O_1- N_ε (H64): 2.83 (Nitrite) O_2- N_ε (H64): 3.20	Crystal soak (PDB entry 2FRF)	38
human Hb (α subunit)-NO_2^-	O-bound	(Nitrite) O_1- N_ε (H58): 2.86 (Nitrite) O_2- N_ε (H58): 3.30	X-ray (PDB entry 3D7O)	39
human Hb (β subunit)-NO_2^-	O-bound	(Nitrite) O_1- N_ε (H63): 2.92 (Nitrite) N- N_ε (H63): 4.10	X-ray (PDB entry 3D7O)	39
cyt cd_1 NiR[c]-NO_2^-	N-bound	(Nitrite) O_2- N_ε (H345): 3.17 (Nitrite) O_2- N_ε (H388): 3.15	X-ray (P DB entry 1AOQ)	40
cyt *c* NiR[d]-NO_2^-	N-bound	(Nitrite) O_1- N_ε (H277): 2.58 (Nitrite) O_1- O (Y218): 3.79 (Nitrite) O_2- N (R114): 2.81	X-ray (P DB entry 2E80)	41

[a] Sperm whale myoglobin; [b] Horse heart myoglobin; [c] From *P. pantotrophus*; [d] From *W. succinogenes*

Dynamics property of nitrite binding to L29H/F43Y Mb

To further probe the dynamic behavior of nitrite binding to L29H/F43Y Mb, we performed two separate MD simulations of L29H/F43Y Mb-nitrite complex for 10 ns as well as control simulations of Mb-nitrite complex under the same condition. As shown in Fig. 4a, the native distal His64 was found to interact with nitrite primarily through hydrogen bonding

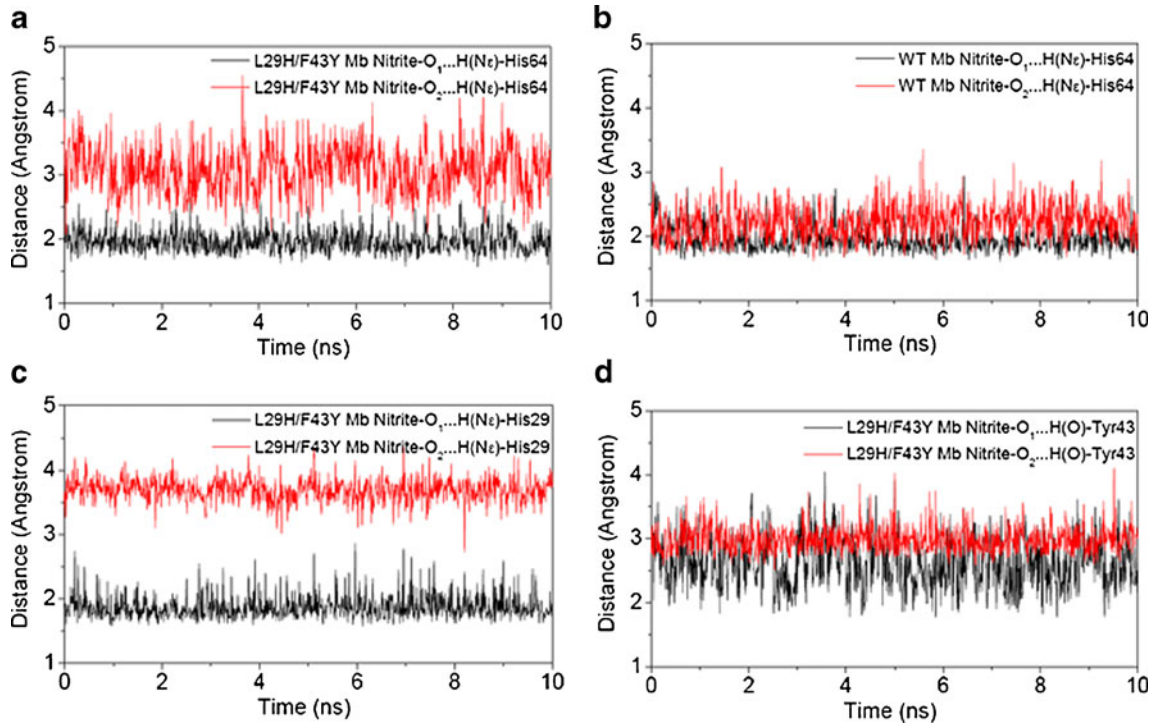

Fig. 4 Time-dependent of hydrogen bonds distances between distal His64 and nitrite ion in L29H/F43Y Mb-nitrite (**a**) and Mb-nitrite (**b**) complexes, and between distal His29 (**c**), tyrosine (**d**) and nitrite ion in L29H/F43Y Mb-nitrite complex

between O_1…H(N_ε-H64) with an average distance of 1.96 Å, where the interaction of O_2…H(N_ε-H64) is comparatively weaker (3.05 Å). In control simulation of Mb-nitrite complex, the average distances extracted from two separate 10 ns MD simulations of the O_1…H(N_ε-H64) and O_2…H(N_ε-H64) bonds are 1.92 Å and 2.28 Å, respectively (Fig. 4b). The distances are close to that from previous 10 ns MD simulation of nitrite binding to human Hb, β subunit, in the O-bound model (1.870 Å and 2.328 Å, respectively) [35]. These observations suggest that the modification of heme pocket alters the dynamics behavior of distal His64, resulting in a weaker nitrite O_2…H(N_ε-H64) interaction for L29H/F43Y Mb-nitrite complex.

As a complement, a stronger hydrogen bonding interaction was observed for distal His29 and nitrite O_2 atom, with an average distance of 1.87 Å, which is slightly shorter than that of nitrite O_1…H(N_ε-H64) (1.96 Å). On the other hand, H(N_ε-H29) can hardly interact with the nitrite O_1 atom (average distance, 3.68 Å), due to the conformation of nitrite in a O-bound model. The hydrogen bonding interactions of nitrite O_1…H(N_ε-H64) and nitrite O_2…H(N_ε-H29) observed for the two distal histidines may potentially play a role in providing the two protons during reduction of NO_2^- to NO.

Additionally, the distal Tyr43 was also found to interact alternatively with both O atoms of nitrite through hydrogen bonding interactions, with an average distance of 2.62 Å and 2.98 Å for nitrite O_1…H(O-Y43) and nitrite O_2…H(O-Y43), respectively. The O_1…H(O-Y43) distance spans a broader range compared to that of O_2…H(O-Y43), suggesting it is a more dynamic hydrogen bond. Moreover, these interactions are slightly weaker in comparison to that of nitrite O_1…H(N_ε-H64) and nitrite O_2…H(N_ε-H29), which agrees with the experimental observations for native cyt *c* NiR-NO_2^- complex (Table 1) [41]. These observations also indicate that the distal Tyr likely plays a different role in nitrite reduction. As shown very recently by Radoul et al., the distal Tyr in cyt cd_1 NiR was found to be crucial for NO formation by interaction with the product [42].

Conclusions

In summary, using molecular modeling combined with dynamics simulation, we rationally designed an artificial NiR based on Mb mimicking cyt cd_1 NiR. As designed, L29H/F43Y Mb shares similar structural features of the heme d_1 active site, i.e., two distal histidines and one distal tyrosine. Moreover, L29H/F43Y Mb provides similar hydrogen interactions with nitrite as that in native NiRs, which could therefore contribute to the NiR activity, although nitrite prefers to bind Mb in an O-bound model. With advantages over native cyt cd_1 NiR, such as having a single heme active center and not forming a dimer, L29H/F43Y Mb will serve as an excellent protein model for structural and functional studies of native NiR and ultimate applications. The progress of these studies will also provide an insight into the relatively low NiR activity of the native Mb in biological systems.

Acknowledgments It is a pleasure to acknowledge Prof. S. G. Sligar and Prof. Yi Lu at University of Illinois at Urbana-Champaign, for their kind gift of sperm whale Mb gene. NAMD and VMD were developed by the Theoretical Biophysics Group in the Beckman Institute for Advanced Science and Technology at the University of Illinois at Urbana-Champaign. This work was supported by the National Natural Science Foundation of China, NSFC (No. 21101091), Hunan Provincial Natural Science Foundation (No. 11JJ4017), and Hunan Provincial Education Foundation (No. 11B105).

References

1. Kendrew JC, Bodo G, Dintzis HM, Parrish RG, Wyckoff H, Phillips DC (1958) Nature 181:662–666
2. Sage JT (1997) J Biol Inorg Chem 2:537–543
3. Lin YW, Wu YM, Liao LF (2012) J Mol Model. 18:1591-1596
4. Lu Y, Berry SM, Pfister TD (2003) Chem Rev 101:3047–3080
5. Watanabe Y, Nakajima H, Ueno T (2007) Acc Chem Res 40:554–562
6. Lu Y, Yeung N, Sieracki N, Marshall NM (2009) Nature 460:855–862
7. Sigman JA, Kwok BC, Lu Y (2000) J Am Chem Soc 122:8192–8196
8. Sigman JA, Kim HK, Zhao X, Carey JR, Lu Y (2003) Proc Natl Acad Sci USA 100:3629–3634
9. Zhao X, Yeung N, Russell BS, Garner DK, Lu Y (2006) J Am Chem Soc 128:6766–6767
10. Yeung N, Lin Y-W, Gao Y-G, Zhao X, Russell BS, Lei L, Miner KD, Robinson H, Lu Y (2009) Nature 462:1079–1082
11. Lin Y-W, Yeung N, Gao YG, Miner KD, Tian S, Robinson H, Lu Y (2010) Proc Natl Acad Sci USA 107:8581–8586
12. Lin Y-W, Yeung N, Gao YG, Miner KD, Lei L, Robinson H, Lu Y (2010) J Am Chem Soc 132:9970–9972
13. Lin Y-W (2011) Proteins 79:679–684
14. Sakurai N, Sakurai T (1998) Biochem Biophys Res Commun 243:400–406
15. Butland G, Spiro S, Watmough NJ, Richardson DJ (2001) J Bacteriol 183:189–199
16. Reimann J, Flock U, Lepp H, Honigmann A, Ädelroth P (2007) Biochim Biophys Acta-Bioenerg 1767:362–373
17. Flock U, Lachmann P, Reimann J, Watmough NJ, Ädelroth P (2009) J Inorg Biochem 103:845–850
18. Watmough NJ, Field SJ, Hughes RJL, Richardson DJ (2009) Biochem Soc Trans 37:392–399
19. Zumft WG (1997) Microbiol Mol Biol Rev 61:533–616
20. Cutruzzolà F, Rinaldo S, Castiglione N, Giardina G, Pecht I, Brunori MN (2009) BioEssays 31:885–891
21. Rinaldo S, Giardina G, Castiglione N, Stelitano V, Cutruzzolà F (2011) Biochem Soc Trans 39:195–200
22. Nurizzo D, Silvestrini MC, Mathieu M, Cutruzzolà F, Bourgeois D, Fülöp V, Hajdu J, Brunori M, Tegoni M, Cambillau C (1997) Structure 5:1157–1171
23. Cutruzzola F, Brown K, Wilson EK, Bellelli A, Arese M, Tegoni M, Cambillau C, Brunori M (2001) Proc Natl Acad Sci USA 98:2232–2237

24. Rinaldo S, Arcovito A, Giardina G, Castiglione N, Brunori M, Cutruzzolà F (2008) Biochem Soc Trans 6:1155–1159
25. Vijgenboom E, Busch JE, Canter GW (1997) Microbiology 143:2853–2863
26. Shiva S, Huang Z, Grubina R, Sun J, Ringwood LA, MacArthur PH, Xu X, Murphy E, Darley-Usmar VM, Gladwin MT (2007) Circ Res 100:654–661
27. Hendgen-Cotta UB, Merx MW, Shiva S, Schmitz J, Becher S, Klare JP, Steinhoff HJ, Goedecke A, Schrader J, Gladwin MT, Kelm M, Rassaf T (2008) Proc Natl Acad Sci USA 105:10256–10261
28. Gladwin MT, Kim-Shapiro DB (2008) Blood 112:2636–2647
29. Hendgen-Cotta UB, Kelm M, Rassaf T (2010) Nitric Oxide 22:75–82
30. Heinecke J, Ford PC (2010) Coord Chem Rev 254:235–247
31. Urayama P, Phillips GN Jr, Gruner SM (2002) Structure 10:51–60
32. Humphrey W, Dalke A, Schulten K (1996) J Mol Graph 14:33–38
33. Kalé L, Skeel R, Bhandarkar M, Brunner R, Gursoy A, Krawetz N, Phillips J, Shinozaki A, Varadarajan K, Schulten K (1999) J Comput Phys 151:283–312
34. MacKerell AD Jr, Bashford D, Bellott M Jr, Dunbrack RL, Evanseck J, Field MJ, Fischer S, Gao J, Guo H, Ha S, Joseph D, Kuchnir L, Kuczera K, Lau FTK, Mattos C, Michnick S, Ngo T, Nguyen DT, Prodhom B, Reiher IWE, Roux B, Schlenkrich M, Smith J, Stote R, Straub J, Watanabe M, Wiorkiewicz-Kuczera J, Yin D, Karplus M (1998) J Phys Chem B 102:3586–3616
35. Perissinotti LL, Marti MA, Doctorovich F, Luque F, Estrin DA (2008) Biochemistry 47:9793–9802
36. Yi J, Heinecke J, Tan H, Ford PC, Richter-Addo GB (2009) J Am Chem Soc 131:18119–18128
37. Springer BA, Sligar SG (1987) Proc Natl Acad Sci USA 84:8961–8965
38. Copeland DM, Soares AS, West AH, Richter-Addo GB (2006) J Inorg Biochem 100:1413–1425
39. Yi J, Safo MK, Richter-Addo GB (2008) Biochemistry 47:8247–8249
40. Willians PA, Fulop V, Garman EF, Saunders NFW, Ferguson SJ, Hajdu J (1997) Nature 389:406–412
41. Einsle O, Messerschmidt A, Huber R, Kroneck PMH, Neese F (2002) J Am Chem Soc 124:11737–11745
42. Radoul M, Bykov D, Rinaldo S, Cutruzzola F, Neese F, Goldfarb D (2011) J Am Chem Soc 133:3043–3055